Micromagnetic modelling of L10-FePt/Ag/L10-FePt pseudo spin valves

P. Ho, R. F. L. Evans, R. W. Chantrell, G. C. Han, G. M. Chow et al.

Related Articles

Fabrication of single-dot planar nano-devices and the application to the exchange bias characterization in nano-pillar devices
Appl. Phys. Lett. 101, 222406 (2012)

Efficient excitation and detection of standing spin wave in Permalloy film: Demonstration of spin wave resonator
Appl. Phys. Lett. 101, 212404 (2012)

Suppression of spin relaxation in rubrene nanowire spin valves
Appl. Phys. Lett. 101, 192403 (2012)

Magnetization dynamics of a MgO-based spin-torque oscillator with a perpendicular polarizer layer and a planar free layer
J. Appl. Phys. 112, 083907 (2012)

Ferrite film growth on semiconductor substrates towards microwave and millimeter wave integrated circuits
App. Phys. Rev. 2012, 9 (2012)

Additional information on Appl. Phys. Lett.

Journal Homepage: http://apl.aip.org/

Journal Information: http://apl.aip.org/about/about_the_journal

Top downloads: http://apl.aip.org/features/most_downloaded

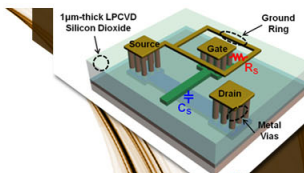Information for Authors: http://apl.aip.org/authors
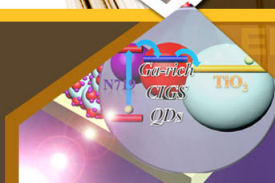
Micromagnetic modelling of $L1_0$-FePt/Ag/$L1_0$-FePt pseudo spin valves

P. Ho,[1,2,a] R. F. L. Evans,[3] R. W. Chantrell,[3] G. C. Han,[2] G. M. Chow,[1] and J. S. Chen[1]

[1]*Department of Materials Science and Engineering, National University of Singapore, Singapore 117576, Singapore*
[2]*Data Storage Institute, Agency of Science, Technology and Research (A*STAR), Singapore 117608, Singapore*
[3]*Department of Physics, University of York, York, United Kingdom*

A micromagnetic bilayer model, based on the Landau-Lifshitz-Bloch equation, was utilized to study the magnetic, reversal, and spin transport properties of MgO/$L1_0$-FePt/Ag/$L1_0$-FePt pseudo spin valves. The model simulates a granular bilayer FePt structure and the effects of the Ag spacer were controlled by varying the interlayer exchange strength. Simulation results showed that the reversal of the FePt layers proceeded via reversed domain formation and propagation. Stray fields emanating from the top soft FePt layer reduced the nucleation field of the bottom FePt locally, resulting in the preferential formation of reversed domains at adjacent sites of the bottom hard FePt layer. © *2011 American Institute of Physics*. [doi:10.1063/1.3653290]

A spin valve consists of a non-magnetic metal sandwiched between two ferromagnets (FMs). Independent switching of the free and fixed layers is ensured by the deliberate creation of larger anisotropy energy (K_u) for the fixed layer or the pinning of the fixed FM using an antiferromagnetic layer. Perpendicular magneto-crystalline anisotropy spin valves have received much attention as they are able to bring about areal density reduction while maintaining thermal stability.[1] High perpendicular anisotropy alloys such as $L1_0$-FePt, with K_u of 7×10^7 erg/cc, are potential candidates for the FM in the spin valves. Recently, MgO/$L1_0$-FePt (20 nm)/Ag (2.5 nm)/$L1_0$-FePt (5 nm) pseudo spin valves (PSVs), with the Ag spacer post-annealed at various temperatures of 300, 400, and 500 °C, have been reported.[2] Post-annealing affects the quality of the FePt/Ag interface, spacer properties, and magnetostatic interactions between the FePt layers, thereby influencing the giant magnetoresistance (GMR).[2–5] In this paper, a micromagnetic bilayer model, based on the Landau-Lifshitz-Bloch (LLB) equation of motion, was utilized to understand the magnetic, reversal, and spin transport properties of these $L1_0$-FePt based PSVs. Conventional micromagnetic calculations for spin systems lack the correct description of the temperature effects because of the assumption of a constant magnetization length. An alternative approach using the LLB equation to study the dynamics of the macrospin system takes into account the longitudinal relaxation processes, important for the magnetization dynamics of high anisotropy materials.[6,7] The LLB equation is given by

$$\vec{m}_i = -\gamma \vec{m}_i \times \vec{H}_{eff}^i - \frac{\gamma \alpha_\perp}{m_i^2} \vec{m}_i \times \left(\vec{m}_i \times \vec{H}_{eff}^i \right) + \frac{\gamma \alpha_{//}}{m_i^2} \left(\vec{m}_i \times \vec{H}_{eff}^i \right) \vec{m}_i, \quad (1)$$

Where $\vec{m}$ is the spin polarization normalized to its zero-temperature value, γ is the gyromagnetic ratio, $\alpha_\perp$ and $\alpha_{//}$ are the dimensionless longitudinal and transverse damping parameters.

The micromagnetic model simulates a granular bilayer structure, which was representative of the bottom fixed and top free $L1_0$-FePt layers, with intralayer exchange fields of 35 kOe and magnetic anisotropies of 1.39×10^7 and 1.69×10^6 erg/cc, respectively. The simulated bilayer system had dimensions of $1.6 \times 1.6 \times 0.03 \ \mu m^3$. Each FePt layer contained 6400 grains which assumed epitaxial grain growth across the FePt layers. The effects of the Ag spacer were controlled by varying the interlayer exchange strength between the FePt layers. The perpendicular magnetoresistance (MR) of the PSVs was determined based on the difference in the magnetization angle between all the epitaxial grains, using the simple model[8]

$$\sum_1^{6400} \frac{[1 - \cos\phi]}{2}, \quad (2)$$

where $\phi = \theta_{bottom} - \theta_{top}$ is the difference in the average spin moment angle between each epitaxial grain on the adjacent FePt layers. θ is the angle which the average magnetic spin moment makes with the z-axis. It is derived from $\cos^{-1}(m_z)$, where m_z is the unit vector of the resultant magnetization in the z direction. The resultant MR loop generated would not reflect an actual GMR ratio as the calculation here is a very much simplified one that assumed excellent spin accumulation at the FePt/Ag interface, perfect matching of the FePt and Ag

TABLE I. Interlayer exchange strength (S_{inter}), fraction of exchange decoupled grains within the fixed FePt (f_{bottom}), and fraction of exchanged decoupled grains within the free FePt layer (f_{top}) for the simulated PSV-300, PSV-400, and PSV-500.

Sample	S_{inter} (Oe)	f_{bottom}	f_{top}
PSV-300	50	0.25	0.05
PSV-400	400	0.30	0.05
PSV-500	4500	0.32	0.05

[a]Author to whom correspondence should be addressed. Electronic mail: g0900564@nus.edu.sg.
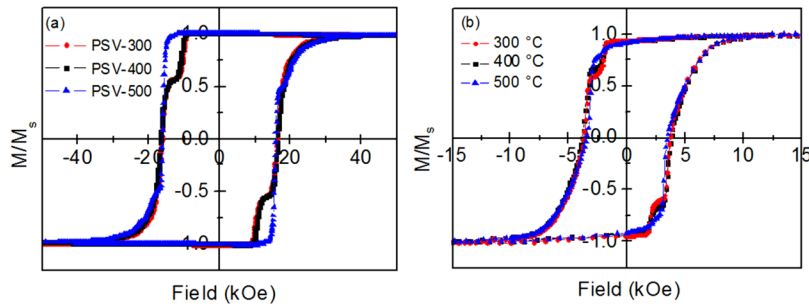
FIG. 1. (Color online) Hysteresis loops of (a) simulated and (b) experimentally fabricated FePt/Ag/FePt PSVs with varying Ag post-annealing temperatures of 300, 400, and 500 °C.

band structures, as well as a defect free crystal with a long spin diffusion length which did not contribute to spin independent flipping. However, the fractional MR values obtained would provide an adequate qualitative comparison of the variation in MR of the PSVs with different Ag post-annealing temperatures. A value of 1 for the fractional MR signifies that all the grains in the bottom FePt are oppositely magnetized with respect to the epitaxial grains in the top FePt.

Previous experimental work reported that the increase in the post-annealing temperature of Ag led to a more extensive FePt/Ag interlayer diffusion.[2] The consequent thinning of the Ag spacer from 2.2 to 1.4 nm when the Ag spacer was post-annealed at 300 and 500 °C, respectively, resulted in the loss of decoupling within the PSV. The interlayer exchange field (S_{inter}) and fraction of exchange decoupled grains within the fixed FePt (f_{bottom}) were varied to simulate the scenario of increased FePt(bottom)/Ag interdiffusion with increasing Ag post-annealing temperature (Table I). The S_{inter} was increased with increasing Ag post-annealing temperature to model the effects of an increasingly thinner Ag spacer. In addition, more extensive Ag diffusion to the high energy grain boundaries is also expected. Hence, higher f_{bottom} values were used to indicate greater grain formation at higher post-annealing temperatures. The fraction of exchanged decoupled grains within the top FePt layer (f_{top}) was maintained at the same value across the PSVs as the experimental deposition temperature of the top FePt layer was unchanged. In this paper, the simulated PSVs with Ag post-annealed at 300, 400, and 500 °C are referred as PSV-300, PSV-400, and PSV-500, respectively.

In our previous work, an atomistic model based on a single grain structure was used to simulate the $L1_0$-FePt/Ag/$L1_0$-FePt PSV system.[2,3] However, experimental results showed that the FePt layers were granular films where lateral intergrain exchange interactions existed. Therefore, a micromagnetic model which uses a multiple grain bilayer structure

with lateral intergrain exchange coupling was used to investigate the PSVs, providing a more accurate representation than the atomistic model. Simulated hysteresis loops [Fig. 1(a)] based on the micromagnetic model show better agreement with experimental results [Fig. 1(b)] compared to the atomistic model.[2,3] The hysteresis loops indicate a gradual decline to magnetization saturation in accordance with the experimental results, instead of an instantaneous reversal at the coercive field in the atomistic model. However, the coercivities obtained for simulated PSVs [Fig. 1(a)] were larger compared to the experimental values [Fig. 1(b)] due to the assumption of a single domain in every grain. Grains in the fabricated samples may be large enough to contain several domains, which would result in a reduction in coercivities. Fig. 1(a) shows that the simulated PSV-300 and PSV-400 were well decoupled but the decoupling between the FePt layers ceased to exist in the simulated PSV-500.

Figures 2(a)–2(d) and 3(a)–3(h) show the configuration snapshots during the reversal process of both the FePt layers for the simulated PSV-300. The reversal mechanism occurred via reversed domain formation (in red) and subsequently domain wall propagation. The reversal mechanism and domain size of the simulated PSV were consistent with those observed experimentally [Figs. 2(e), 3(i), and 3(j)].[9] The top FePt reversed more rapidly and over a narrower switching field distribution. This was attributed to the smaller extent of decoupled grain formation within the top FePt which was not influenced by the bottom FePt/Ag interdiffusion. As such, the reversal of the top FePt occurred more coherently instead of independently as in the case of the more decoupled bottom FePt. In addition, stray fields emanating from the top FePt [Fig. 2(b)] reduced the nucleation field of the bottom FePt locally [Fig. 3(b)], resulting in the preferential formation of reversed domains at the adjacent site on the bottom FePt. These nucleation sites subsequently became the centre for further reversed domain
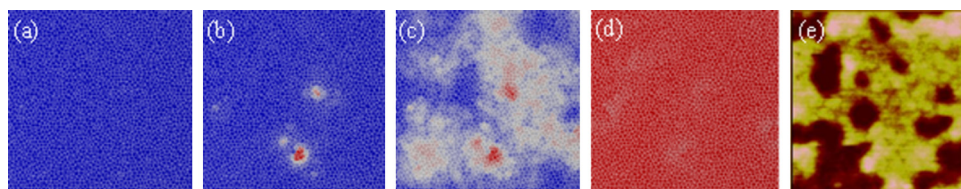

FIG. 2. (Color online) Magnetization configurations of the top FePt layer, with a cross section of $1 \times 1\ \mu m^2$, at an applied field of (a) −10, (b) −11, (c) −12, and (d) −14 kOe for the simulated PSV-300. Reversed domains nucleate and propagate. (e) $1 \times 1\ \mu m^2$ AFM image illustrating the magnetization configurations of the top FePt layer at an applied field of −2 kOe for the experimentally fabricated PSV with Ag post-annealed at 300 °C. Bright regions represent the reversed domains.
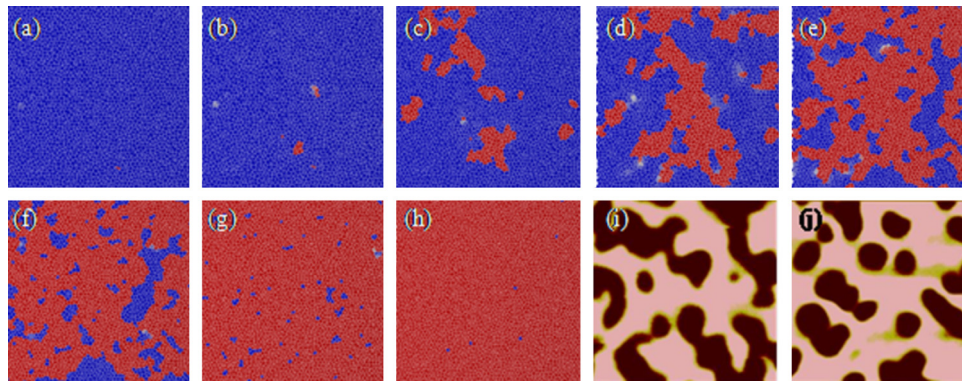
FIG. 3. (Color online) Magnetization configurations of the bottom fixed FePt layer, with a cross section of $1 \times 1 \ \mu m^2$, at an applied field of (a) -10, (b) -12, (c) -17, (d) -18, (e) -19, (f) -20, (g) -30, and (h) -50 kOe for the simulated PSV-300. Reversed domains nucleate and propagate. $1 \times 1 \ \mu m^2$ AFM image illustrating the magnetization configurations of the top FePt layer at an applied field of (i) -4 and (j) -6 kOe for the experimentally fabricated PSV with Ag post-annealed at 300 °C. Bright regions represent the reversed domains.

propagation with increasing negative applied field. Similar reversal mechanism and stray field effects were observed for the simulated PSV-500. Reversal of the top soft FePt layer also proceeded more rapidly than the bottom hard FePt layer. This is an indication that even though the FePt layers appeared to be coupled on the hysteresis loop for the simulated PSV-500, the increased coupling strength due to the thinner Ag spacer was not sufficiently strong enough to result in the concurrent reversal of both FePt layers.

Figure 4 shows the calculated MR of the simulated PSV-300 and PSV-500. The fractional MR of the PSVs decreased from 0.964 to 0.309 with an increase in Ag post-annealing temperature from 300 to 500 °C. On the other hand, the simulated MR loop for the PSV-400 (not shown here) was similar to that of PSV-300, only with a slightly smaller fractional MR of 0.952. These trends were in line with observations made of the current-in-plane MR in the fabricated PSVs.[2] For the simulated PSV-500, the considerable decrease in fractional MR was attributed to the larger number of epitaxial grains in both FePt layers possessing magnetization of identical configurations, due to the significant increase in interlayer exchange coupling between the FePt layers. However, a small MR was still present despite the absence of interlayer decoupling as the reversal of both FePt layers did not occur concurrently. In addition, the increase in MR set in at a much larger applied field as the coercive field of the softer top FePt layer increased due to
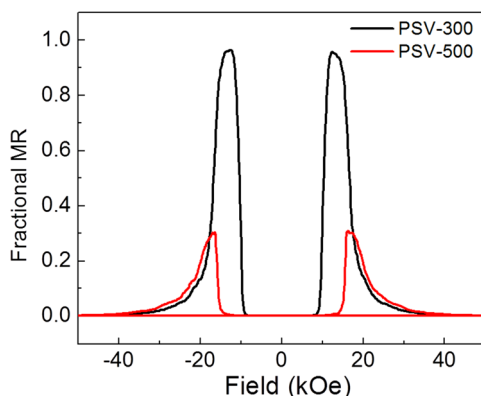
the exchange interaction with the harder bottom FePt layer. The decline in the MR with increasing applied field also occurred more gradually as the increase in the fraction of decoupled grains in the bottom FePt layer reduced the inter-grain exchange coupling and promoted more independent reversal amongst grains. As such, reversal of the bottom FePt layer and the consequent reduction in MR occurred more gradually over a broader range of applied field.

In summary, a micromagnetic bilayer model based on the LLB equation was utilized to study the magnetic, reversal, and MR properties of the $L1_0$-FePt/Ag/$L1_0$-FePt PSVs with the Ag spacer post-annealed at 300, 400, and 500 °C. Simulation results indicate that the reversal of both the FePt layers occurred via reversed domain formation and propagation, in both the absence and presence of exchange decoupling of the FePt layers. It was also evident that dipolar stray field coupling was one of the contributing sources of inter-layer magnetostatic interactions in the PSVs. The MR of the PSV was also shown to decrease with increasing Ag post-annealing temperature due to the increase in interlayer exchange coupling strength as a result of the thinner Ag spacer layer.

FIG. 4. (Color online) Magnetoresistance loops of the simulated PSV-300 and PSV-500.

[1] J. G. Zhu, IEEE. Trans. Magn. **96**, 1786 (2008).
[2] P. Ho, G. C. Han, R. F. L. Evans, R.W. Chantrell, G. M. Chow, and J. S. Chen, Appl. Phys. Lett. **98**, 132501 (2011).
[3] P. Ho, G. C. Han, R. F. L. Evans, R.W. Chantrell, G. M. Chow, and J. S. Chen, IEEE Trans. Magn. (in press).
[4] E. M. Ho, A. K. Petford-Long, and A. Cerezo, J. Magn. Magn. Mater. **192**, 431 (1999).
[5] C. L. Zha, J. Nogues, and J. Akerman, IEEE. Trans. Magn. **45**, 3881 (2009).
[6] M. Hartl-Malang, J. Kotzler, and D. A. Garanin, Phys. Rev. B **51**, 8974 (1995).
[7] N. Kazantseva, D. Hinzke, U. Nowak, R. W. Chantrell, U. Atxitia, and O. Chubykalo-Fesenko, Phys. Rev. B **77**, 184428 (2008).
[8] B. A. Gurney, M. Carey, C. Tsang, M. Williams, S. S. P. Parkin, R. E. Fontana, Jr., E. Grochowski, M. Pinarbasi, T. Lin, and D. Mauri, *Ultrathin Magnetic Structures IV*, edited by B. Heinrich and J. A. C. Bland (Springer, Berlin, 2005), Chap. 6, p. 2.
[9] P. Ho, G. C. Han, G. M. Chow, and J. S. Chen, Appl. Phys. Lett. **98**, 252503 (2011).